# Longwave Scattering Effects of Mineral Aerosols

JEAN-LOUIS DUFRESNE,* CATHERINE GAUTIER,+ AND PAUL RICCHIAZZI

*Institute for Computational Earth System Science, University of California at Santa Barbara, Santa Barbara, California*

YVES FOUQUART

*Laboratoire d'Optique Atmosphérique, CNRS-Université de Lille, Villeneuve d'Ascq, France*

(Manuscript received 4 September 2001, in final form 26 November 2001)

## ABSTRACT

Scattering in the longwave domain has been neglected in the first generation of radiative codes and is still neglected in most current GCMs. Scattering in the longwave domain does not play any significant role for clear-sky conditions but recent works have shown that it is not negligible for cloudy conditions. This paper highlights the importance of scattering by mineral aerosols in the longwave domain for a wide range of conditions commonly encountered during dust events. The authors show that neglecting scattering may lead to an underestimate of longwave aerosol forcing. This underestimate may reach 50% of the longwave forcing at the top of atmosphere and 15% at the surface for aerosol effective radius greater than a few tenths of a micron. For an aerosol optical thickness of one and for typical atmospheric conditions, the longwave forcing at the top of the atmosphere increases to 8 W m$^{-2}$ when scattering effects are included. In contrast, the heating rate inside the atmosphere is only slightly affected by aerosol scattering: neglecting it leads to an underestimate by no more than 10% of the cooling caused by aerosols.

## 1. Introduction

Observations and models highlight the importance of radiative forcing by mineral aerosols on the earth's energy budget (Haywood and Boucher 2000). Aerosol scattering and absorption of solar radiation reduces the flux absorbed by the surface, especially over dark regions such as oceans, while aerosol absorption and scattering in the longwave enhances the greenhouse effect. These opposing mechanisms are of the same order of magnitude, and mineral aerosols have been found to produce either a positive (Tegen et al. 1996) or negative net forcing (Miller and Tegen 1998; Hansen et al. 1998). A precise computation of the radiative exchanges is thus required in both the shortwave and the longwave domain. Previous studies have investigated the aerosol parameters that have the greatest impact on radiative forcing. For example Claquin et al. (1998), Liao and Seinfeld (1998), Sokolik and Golitsyn (1993), Schulz et al. (1998), and Sokolik and Toon (1999) have addressed

how the dust size distribution, the mineral properties, the mineral composition and the vertical distribution of aerosol affect the radiative exchanges. In this study we focus on the importance of scattering in the longwave domain (from 4 to 100 $\mu$m).

Scattering in the longwave may be important if the two following conditions are satisfied: the reflectivity of the aerosol layer is significant and the distribution of the longwave radiative sources is very anisotropic (Fouquart et al. 1990). This last condition is verified in spectral regions where the gas absorption is small. Indeed, if the gas is perfeclty transparent, the upward flux is the flux emitted by the surface whereas the downward flux is zero. On Mars for example, the atmosphere is transparent in most of the longwave domain and scattering by dust particles is important (Toon et al. 1989; Forget et al. 1999). Scattering in a pristine clear atmosphere is unimportant as Rayleigh scattering is small in the longwave. For cloudy conditions, the droplet absorption dominates, the reflectivity is very low and a commonly used assumption is to consider cloud droplets as purely absorbing particles (Fouquart et al. 1990). But the longwave scattering effect may have to be taken into account if greater precision is required. The importance of scattering effect has been shown for water clouds (Ritter and Geleyn 1992; O'Brien et al. 1997; Fu et al. 1997) and for cirrus clouds (Liou 1986; Ritter and Geleyn 1992; Edwards and Slingo 1996; Fu et al. 1997). For water clouds, scattering is important in the atmospheric

---

window, between 8 and 13 $\mu$m (850–2100 cm$^{-1}$) (O'Brien et al. 1997; Takara and Ellingson 2000). For cirrus clouds the spectral domain near 25 $\mu$m (400 cm$^{-1}$) is also important, especially for cold subarctic winter conditions (Edwards and Slingo 1996). One reason is the existence of a transparent window near 25 $\mu$m (400 cm$^{-1}$) due to the very low water vapor content at these high altitudes.

Submicron aerosols, like sulfate aerosols, are too small to play a significant role in the longwave radiative exchanges. Dust aerosols have a larger radius and may be more important (Sokolik et al. 1998). Fouquart et al. (1987) found that the scattering effect has little impact ($\approx 1$ W m$^{-2}$) in a dust storm case where the retrieved aerosols size was small. But to the best of our knowledge, the possible importance of scattering in the longwave has not yet been quantified in the general case.

## 2. Radiative model and radiative properties

In the present study we use the SBDART code (Ricchiazzi et al. 1998) to compute atmospheric radiative transfer in the longwave domain (from 4 to 100 $\mu$m). This program incorporates low-resolution band models developed for LOWTRAN7 (Pierluissi and Peng 1985), and uses a discrete ordinate method (DISORT, Stamnes et al. 1988) to integrate the radiative transfer equation. The 20-cm$^{-1}$ spectral resolution is sufficient to study the effect of particles that do not have sharp spectral lines (e.g., O'Brien et al. 1997). The atmosphere is divided into 50 vertical layers and we use the five standard atmospheric vertical profiles (McClatchey et al. 1972) commonly used for radiative transfer studies: tropical, midlatitude summer, midlatitude winter, subarctic summer, and subarctic winter. We also add a "dry tropical" atmosphere by reducing the humidity of the tropical atmosphere by a factor of two. The surface emissivity is one, as is appropriate over the ocean surface.

For aerosol refractive index, we use the so-called "Barbados Sahara dust" properties (Sokolik et al. 1998), which were measured by Volz (1973) and used by many authors (e.g., Carlson and Benjamin 1980; d'Almeida 1987; Tegen et al. 1996). The size of dust aerosols varies over two orders of magnitude. Near aerosol sources, particle radius distribution display three main modes (Gomes et al. 1990) a submicron particle mode and modes around 3 $\mu$m and 60 $\mu$m. This wide range of particle radius has been considered by various GCMs studies (e.g., d'Almeida 1987; Schulz et al. 1998). Here, we consider that the radius has a lognormal distribution with a geometric standard deviation $\sigma_g = 2$ and we follow Tegen and Lacis (1996) by considering particles with an effective radius ranging from 0.1 $\mu$m to 10 $\mu$m. The dust particles may have various shapes. The assumption of sphericity may lead to important errors when computing the radiance but should not produce significant errors when computing radiative fluxes (Mishchenko et al. 1995; Lacis and Mishchenko 1995).
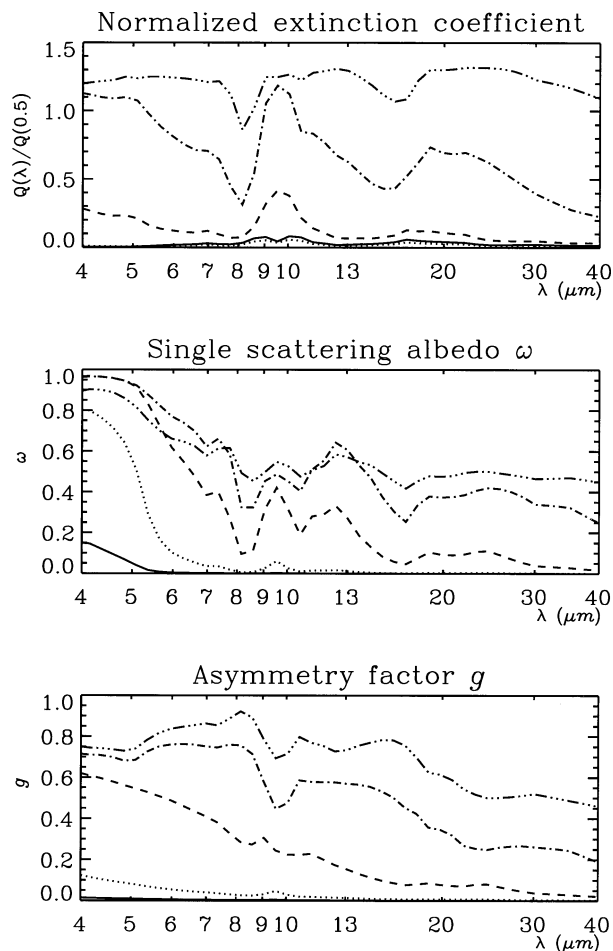


FIG. 1. Wavelength dependence of normalized extinction coefficient, single scattering albedo, and asymmetry for six effective radii: 0.1 (solid), 0.3 (dot), 1 (dash), 3 (dash–dot), and 10 (dash–dot-dot-dot). The extinction coefficient is normalized by its value at 0.5 $\mu$m.

Because our study is mainly concerned with fluxes, we make the common assumption of sphericity for the dust particles and use a Mie code (Wiscombe 1980) to compute their optical properties. Unlike the rather smooth behavior in the shortwave, in the longwave there are strong variations in aerosol optical parameters as the effective radius is varied between 0.5 $\mu$m and 10 $\mu$m (e.g., Tegen and Lacis 1996). Over this range of particle size, the extinction coefficient $Q_{ext}$ increases strongly, as the single scattering albedo ramps up from near 0 to 0.5, and the asymmetry factor increases from about 0 (isotropic scattering) up to near 1 (forward scattering dominates; Fig. 1).

## 3. Results

We compute the aerosol longwave radiative forcing with and without scattering. In the latter case, the absorption approximation is used: the extinction coefficient is set to the absorption coefficient value and the single
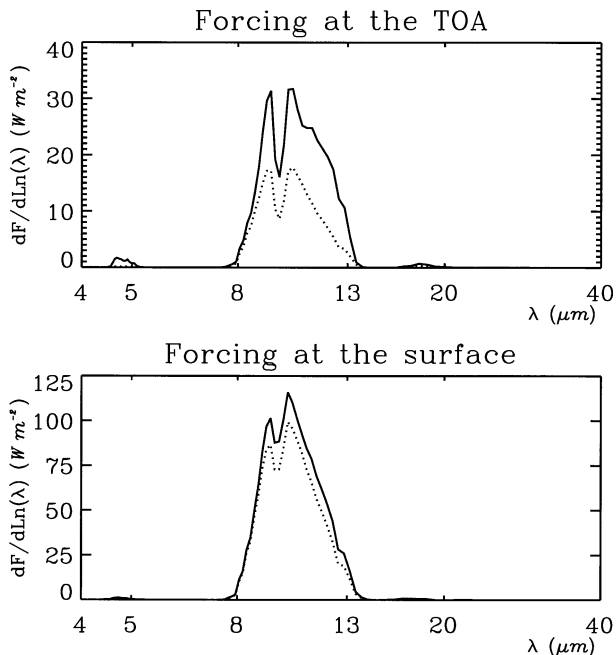
## Forcing at the TOA



## Forcing at the surface



FIG. 2. Wavelength dependence $dF/d \ln(\lambda)$ of the aerosol radiative forcing $F$ at TOA (top) and at surface (bottom) as a function of the logarithm of the wavelength $\lambda$, for the dry tropical atmospheric profile and for an homogeneous aerosol layer extending from the surface up to 3-km height. The aerosol effective radius is 2 $\mu$m and the optical thickness at 500 nm is 1. Computation is either exact (solid line) or neglects scattering (dotted line). We use a logarithmic scale for the $\lambda$ axis. The total area under the curve of $dF/d \ln(\lambda)$ indicates the total power. Here, $dF/d\lambda$ in W m$^{-2}$ $\mu$m$^{-1}$ may be obtained using the relation $dF/d \ln(\lambda) = \lambda dF/d\lambda$.

scattering albedo is set to 0. We consider a simple atmospheric situation which approximates dust storm conditions: a dry tropical atmospheric profile with a homogeneous aerosol concentration from the surface to a 3-km height and an aerosol effective radius of 2 $\mu$m. The wavelength dependence of the aerosol radiative forcing at the top of the atmosphere (TOA) and at the surface displays well-known characteristics (Fig. 2). The radiative forcing is significant only in the atmospheric window, between 8 and 13 $\mu$m. At the surface, the forcing

## Aerosol forcing $F$



## Aerosol forcing error $\epsilon_F$

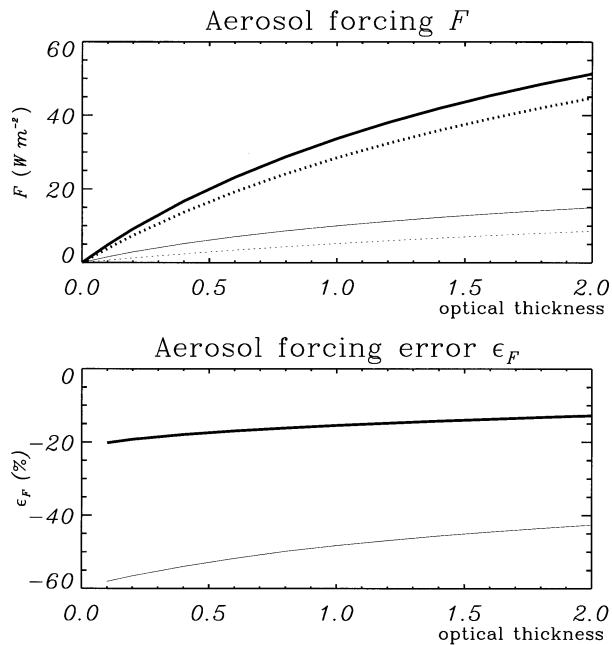

FIG. 3. (top) Aerosol radiative forcing at TOA (thin lines) and at surface (thick lines) as a function of aerosol optical thickness at 0.5 $\mu$m considering (solid) or neglecting (dotted) scattering. All other conditions are the same as in Fig. 2. (bottom) Relative error in radiative forcing due to the neglect of scattering at the TOA (thin lines) and at the surface (thick lines).

is important relative to the radiative budget (Table 1, Fig. 2). Indeed the downward flux in the atmospheric window is almost zero for clear-sky conditions, whereas it is dramatically increased by aerosol emission in dusty conditions. At the TOA, the overall effect of aerosol is to reduce the outgoing longwave radiation. Absorption and scattering by aerosols reduce the flux emitted by the surface that directly leaves the top of the atmosphere. This flux decrease is not compensated by the flux increase due to aerosol emission, as the aerosol temperature is lower than the surface temperature.

Neglecting scattering causes an error of approximately the same magnitude at the TOA and at the surface, which amounts to ≈5 W m$^{-2}$ in the previous ex-

TABLE 1. Aerosol longwave radiative forcing at the TOA and at the surface, for the six atmospheric profiles considered in the text. Same aerosol conditions as in Fig. 2.

| Atmospheric profile | Longwave forcing at the TOA | | | | Longwave forcing at the surface | | | |
|---|---|---|---|---|---|---|---|---|
| | Exact (W m$^{-2}$) | Neglecting scattering (W m$^{-2}$) | Error (W m$^{-2}$) | Relative error (%) | Exact (W m$^{-2}$) | Neglecting scattering (W m$^{-2}$) | Error (W m$^{-2}$) | Relative error (%) |
| Tropical | 7.4 | 3.9 | −3.5 | −48 | 21.2 | 17.7 | −3.5 | −16 |
| Dry tropical | 10.2 | 5.3 | −4.9 | −48 | 34.4 | 29.1 | −5.3 | −15 |
| Middle latitude summer | 7.5 | 3.7 | −3.9 | −51 | 26.6 | 22.5 | −4.1 | −15 |
| Middle latitude winter | 6.9 | 3.0 | −3.8 | −56 | 31.7 | 27.2 | −4.5 | −14 |
| Artic summer | 8.2 | 4.3 | −3.9 | −47 | 29.3 | 24.9 | −4.5 | −15 |
| Artic winter | 3.5 | 0.4 | −3.1 | −88 | 29.4 | 25.7 | −3.7 | −13 |
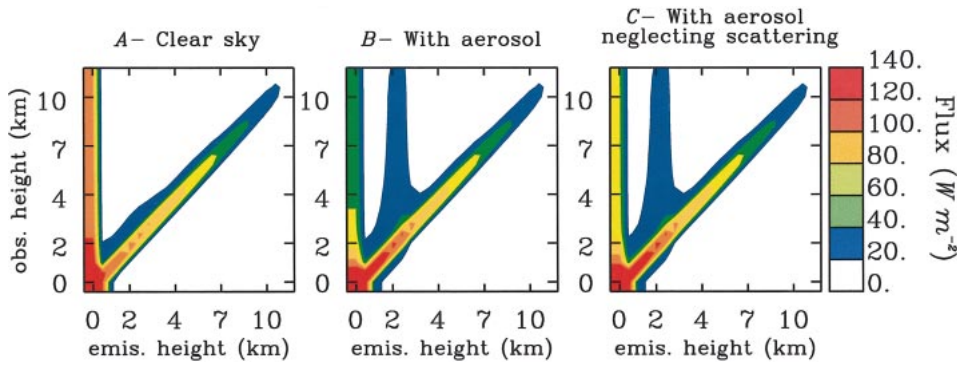
FIG. 4. Contour plot displaying how the irradiance (in W m$^{-2}$) emitted by a layer is a function of the altitude where the radiation is observed (vertical axis) and of the altitude where the radiation has been emitted (horizontal axis). Both altitudes are in km. The atmosphere is clear in (a), aerosol are present in (b), and aerosol are present but scattering is neglected in (c). Same aerosol and atmospheric conditions as in Fig. 2.

ample (Fig. 2). This corresponds to a small relative error for the longwave forcing at the surface ($\approx 15\%$), but to an error as large as $\approx 50\%$ for the longwave forcing at the TOA. These relative errors are almost independent of the aerosol optical thickness (Fig. 3). Results are not very sensitive to the atmospheric vertical profile, the error ranging from 3 to 5 W m$^{-2}$ (Table 1). For winter conditions, and especially for arctic winter conditions, the aerosol forcing is also present in the spectral region around 20 $\mu$m, and the relative error on longwave ra-
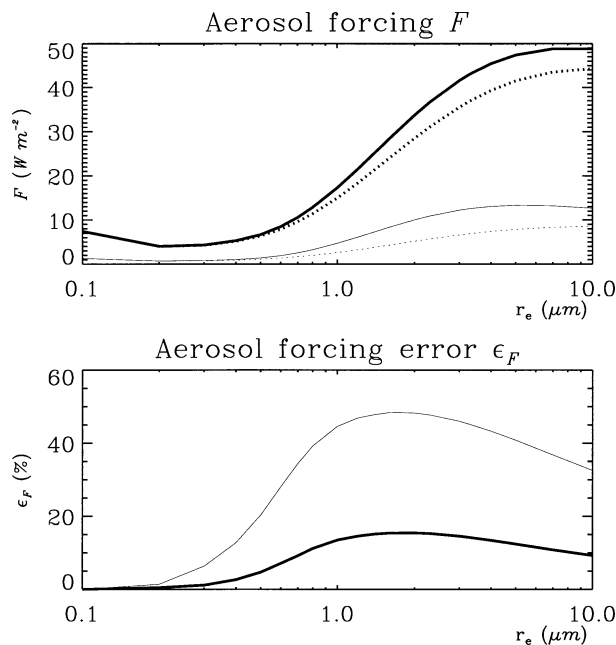


FIG. 5. (top) Aerosol radiative forcing at TOA (thin lines) and at surface (thick lines) as a function of aerosol effective radius $r_e$ considering (solid) or neglecting (dotted) scattering. All other conditions are the same as in Fig. 2. (bottom) Relative error in radiative forcing due to the neglect of scattering at the TOA (thin lines) and at the surface (thick lines).

diative forcing at the TOA when neglecting scattering jumps to 90%.

Figure 4 illustrates how aerosol absorption, emission, and scattering modify the radiative exchange. The flux of photons incident on a layer are shown as a function of the layer altitude from which they were emitted. This diagnostic can be directly obtained with Monte Carlo codes. With a discrete ordinate code like SBDART, the diagnostic was approximated by perturbing separately the temperature of each layer. Photons emitted in the strongly absorbing regions of the longwave spectrum have a very short pathlength, and thus are absorbed close to where they are emitted, creating the diagonal band seen in Fig. 4. However, in the atmospheric window region where absorption is low, photons emitted by the surface leave the atmosphere directly, as indicated by the vertical colored column at the left of Fig. 4a. When aerosols are present (Fig. 4b), the flux emitted by the surface decreases with height much more rapidly than in clear-sky conditions, due to aerosol absorption and scattering, and only a small fraction reaches the TOA. On the other hand, the flux emitted inside the dust layer takes on greater importance. At the top of the dust layer, where the optical depth is small, the emitted flux can reach the TOA, as illustrated by the vertical colored column at a height around 2 km. The neglect of scattering (Fig. 4c) mainly reduces the attenuation of the flux emitted by the surface, allowing more of the surface flux to reach the TOA. The radiative exchange inside the atmosphere displays no qualitative important change when scattering is neglected.

For the same conditions as in Fig. 2, and keeping constant the optical thickness in the visible (at 500 nm), we explore the effect of changing the effective radius over the range 0.1–10 $\mu$m (Fig. 5). The aerosol radiative forcing both at TOA and at surface strongly increases as the effective radius increases from 0.5 $\mu$m to 5 $\mu$m. When aerosol forcing is significant, the error due to

## Aerosol forcing F
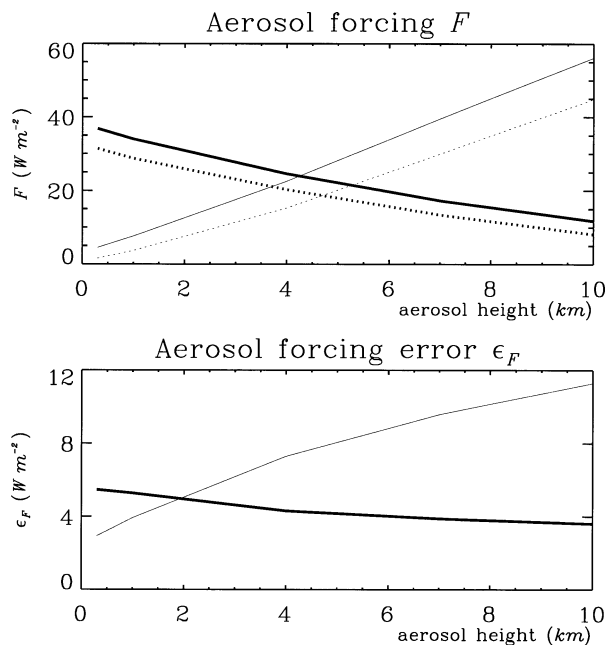


## Aerosol forcing error $\epsilon_F$



FIG. 6. (top) Aerosol radiative forcing at TOA (thin lines) and at surface (thick lines) as a function of aerosol layer altitude (in km), considering (solid) or neglecting (dot) scattering. The aerosol layer is 500 m thick, the effective radius is 2 $\mu$m, the optical thickness at 500 nm is 1, and the atmosphere corresponds to a dry tropical profile. (bottom) Error due to the neglect of scattering forcing at TOA (thin lines) and at surface (thick lines), for the same conditions.

neglecting scattering is also significant and has about the same value at the TOA and at the surface.

The dependence of radiative forcing at the TOA and surface due to variation of aerosol temperature are almost proportional but of opposite sign (Fig. 6). In dust storm conditions, where aerosols are well mixed in the lower few kilometers of the atmosphere, the longwave forcing at the surface dominates (Figs. 2 and 5). Far from the sources, aerosols may be located in a relatively thin layer at a few kilometers height, like the so-called Saharan Air Layer, and the longwave radiative forcing at the TOA and at the surface become comparable. In dust storm conditions, the error due to the neglect of scattering is almost the same for the forcing at the surface and TOA (Table 1). But for a thin aerosol layer, the error in forcing at the surface remains constant with aerosol altitude, whereas the error increases for forcing at the TOA (Fig. 6). The reasons will be explained later.

Longwave radiation creates a strong cooling in the upper part of the aerosol layer (Carlson and Benjamin 1980; Fouquart et al. 1987; Quijano et al. 2000). Our results display the same cooling but with a sharper profile due to an enhanced vertical resolution (Fig. 7). In the atmospheric window, aerosols loose more energy by emission than they gain from absorbing radiation emitted by the surface. Outside the atmospheric window, aerosols do not modify the cooling rate. Scattering does not play any significant role as far as the heating rate
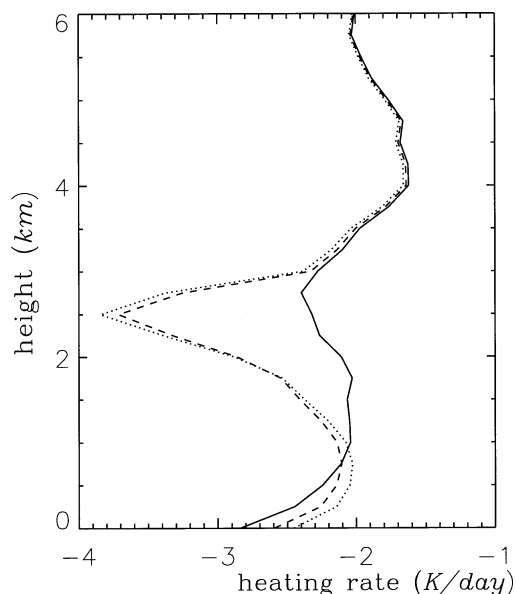


FIG. 7. Longwave heating rate for the dry tropical atmospheric profile in clear-sky conditions (solid line), with aerosols (dotted line) or with aerosols but ignoring scattering (dashed line). Same aerosol conditions as in Fig. 2.

inside the atmosphere is concerned: neglecting scattering only slightly reduces the cooling at top of the aerosol layer, whereas it slightly increases the cooling at the bottom (Fig. 7).

## 4. Simple conceptual model

It is possible to develop a simplified model that explains the main results generated by SBDART. In the case of a homogeneous isothermal aerosol layer, the upward spectral irradiance above the layer is given by (e.g., Edwards and Slingo 1996)

$$F_t^+ = (1 - A - R)F_b^+ + RF_t^- + A\pi B, \qquad (1)$$

where $F^+$ and $F^-$ are, respectively, the upward and downward irradiance, and $B$ is the Planck irradiance at the aerosol temperature. The suffixes $b$ and $t$ indicate the irradiance values at the bottom or top of the aerosol layer. Parameters $A$ and $R$, the absorption and reflection coefficients of the aerosol layer, can be expressed using the hemispheric mean approximation as a function of the aerosol optical thickness $\tau$, the single scattering albedo $\omega$, and the asymmetry factor $g$:

$$A = (1 - \omega)\tau, \quad \text{and} \qquad (2)$$

$$R = \frac{\omega}{2}(1 - g)\tau. \qquad (3)$$

The radiative forcing $\delta F_t^+$ above the aerosols, that is, the opposite of the change of irradiance $F_t^+$ due to the presence of aerosols, can be written as,

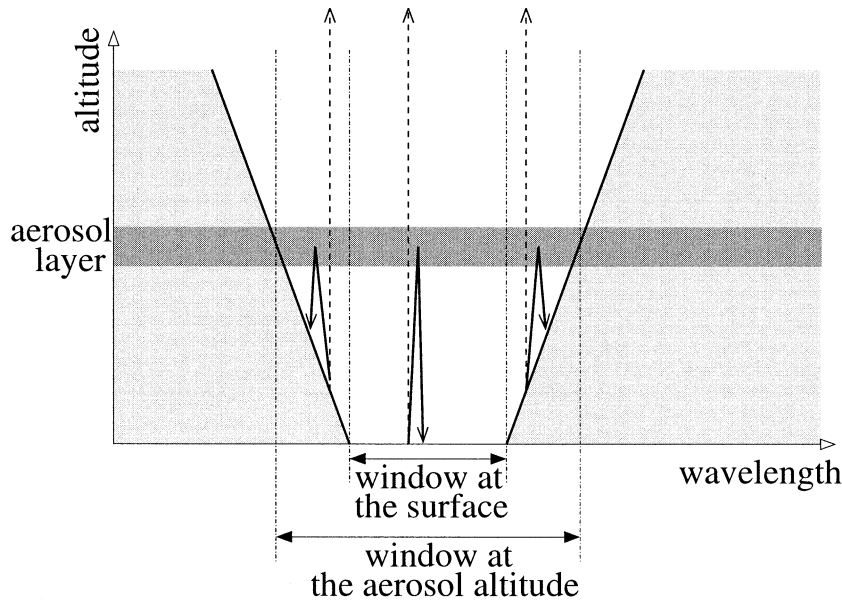$$\delta F_t^+ = A(F_b^+ - \pi B) + R(F_b^+ - F_t^-). \qquad (4)$$

FIG. 8. Schematic representation of how the longwave radiative properties of the atmosphere depend on wavelength and altitude. The atmosphere is opaque in the light gray region and transparent in the white region. The bulk of the energy transport is carried by photons, which are emitted by the surface or at the transition between the opaque and transparent regions. Photons that are backscatter by aerosols in an exact computation (solid arrows) reach the TOA when scattering is neglected (dashed arrows).

In the spectral region of strong gas absorption, $F_b^+ \approx F_t^- \approx \pi B$, which leads to an aerosol forcing almost equal to zero, whether or not scattering by aerosols is considered. Hence, aerosol forcing outside the atmospheric window is negligible (Fig. 2). In the spectral regions where the gas is perfectly transparent, the upward irradiance $F_b^+$ at the bottom of the aerosol layer is equal to the upward irradiance $F_s^+$ above the surface, and the downward irradiance $F_t^-$ at the top of the aerosol layer is zero. The aerosol radiative forcing is

$$\delta F_t^+ = A(F_s^+ - \pi B) + RF_s^+. \tag{5}$$

The same calculation for the forcing at the surface in the window region yields

$$\delta F_b^- = A\pi B + RF_s^+. \tag{6}$$

The first term of the right-hand side of Eqs. (5) and (6) corresponds to the monochromatic irradiance absorbed and/or emitted by aerosols. The dependence of forcing at the TOA and surface versus aerosol temperature are both proportional to the absorption coefficient $A$ but of opposite sign, as previously found in Fig. 6. Radiative forcing at the TOA is more sensitive to surface temperature change than the radiative forcing at the surface. Indeed, the first is proportional to $A + R$, whereas the second is proportional to $R$ [Eqs. (5) and (6)]. For typical conditions, $(A + R)/R$ is about 5.

The second term of the right-hand side of Eqs. (5) and (6) corresponds to aerosol scattering. It represents the monochromatic flux emitted by the surface and backscattered by the aerosol layer. When we consider a thin aerosol layer at different altitudes, the error due to neglecting scattering is almost constant for the forcing at the surface but increases with the aerosol altitude for the forcing at the TOA (Fig. 6). The schematic diagram shown in Fig. 8 helps to explain these results. For forcing at the surface, the error due to the neglect of scattering depends on the width of the atmospheric window near the surface and thus is independent of the aerosol altitude. For forcing at the TOA, the error depends on the width of the atmospheric window at the aerosol altitude. When the aerosol altitude increases, the local water vapor content decreases and the width of the atmospheric window increases. Thus the error due to the neglect of scattering also increases.

When the aerosol temperature approaches the surface temperature ($F_s^+ \approx \pi B$), the radiative forcing equations can be simplified even further. Aerosol forcing at the TOA is produced only by scattering [see Eq. (5)] and neglecting it yields up to a 100% error. At the surface, the relative error $\epsilon_s$ due to neglecting scattering becomes $\epsilon_s \approx R/(A + R)$. If the aerosol optical thickness is small ($\tau < 1$), which is often the case for mineral dust, the optically thin approximation allows the relative error in the whole atmospheric window to be written as,

$$\overline{\epsilon}_s = \frac{\int_\lambda \frac{\omega}{2}(1 - g)Q_{\text{ext}} \, d\lambda}{\int_\lambda \left(1 - \frac{\omega}{2}(1 + g)\right)Q_{\text{ext}} \, d\lambda}. \tag{7}$$

Computing the above expression in the wavelength interval 8–13 $\mu$m reproduces the main characteristic of the dependency of scattering error versus aerosol radius as computed by SBDART.

## 5. Conclusions

Previous research has emphasized the importance of having a good representation of effective radius, mineral composition and vertical aerosol profile for a good estimate of dust–aerosol radiative forcing. In this work we focus on the longwave spectral domain and we highlight the importance of scattering for a wide range of conditions commonly encountered during dust events. When the effective radius is greater then a few tenths of a micron, scattering contributes to longwave forcing at the TOA at a level of 20% to 60%. Scattering has less impact on surface forcing (about 5% to 20%) and has negligible impact on atmospheric heating rate. These relative errors do not depend on the aerosol optical thickness but mainly on the aerosol size distribution and aerosol refractive index.

The use of a very simplified model allows us to interpret the radiative forcing and its sensitivity to key atmospheric parameters. The main effect of scattering is to backscatter the upwelling flux emitted by the surface, and this is only important in the atmospheric window region, between 8 and 13 $\mu$m. Scattering has more impact on the forcing at the TOA for a thin aerosol layer at high altitude than for a well-mixed aerosol layer just above the surface. In current studies investigating the climate effect of mineral aerosols, scattering in the longwave domain may be considered (e.g., Toon et al. 1989; Hansen et al. 1983) or neglected (e.g., Lacis and Mishchenko 1995; Claquin et al. 1998). Neglecting longwave scattering may lead one to underestimate the longwave radiative forcing of mineral aerosols. Though this study did not address the global climate impact of this underestimate, the results show that longwave scattering must be taken into account when longwave aerosol forcing is significant compared to other radiative forcings.

### REFERENCES

Carlson, T., and S. Benjamin, 1980: Radiative heating rates for Saharan dust. *J. Atmos. Sci.,* **37,** 193–213.

Claquin, T., M. Schulz, Y. Balkanski, and O. Boucher, 1998: Uncertainties in assessing radiative forcing by mineral dust. *Tellus,* **50B,** 491–505.

d'Almeida, G., 1987: On the variability of desert aerosol radiative characteristics. *J. Geophys. Res.,* **92,** 3017–3026.

Edwards, J., and A. Slingo, 1996: Studies with a flexible new radiation code. I. Choosing a configuration for a large-scale model. *Quart. J. Roy. Meteor. Soc.,* **122,** 689–719.

Forget, F., and Coauthors, 1999: Improved general circulation models of the Martian atmosphere from the surface to above 80 km. *J. Geophys. Res.,* **104,** 24 155–24 175.

Fouquart, Y., B. Bonnel, G. Brogniez, J. Buriez, L. Smith, J. Morcrette, and A. Cerf, 1987: Observations of Saharan aerosols: Results of ECLATS field experiment. Part II: Broadband radiative characteristics of the aerosols and vertical radiative flux divergence. *J. Climate Appl. Meteor.,* **26,** 38–52.

——, J. Buriez, M. Herman, and R. Kandel, 1990: The influence of clouds on radiation: A climate-modeling perspective. *Rev. Geophys.,* **28,** 145–166.

Fu, Q., K. Liou, M. Cribb, T. Charlock, and A. Grossman, 1997: Multiple scattering parameterization in thermal infrared radiative transfer. *J. Atmos. Sci.,* **54,** 2799–2812.

Gomes, L., G. Bergametti, G. Coude-Gaussen, and P. Rognon, 1990: Submicron desert dusts: A sandblasting process. *J. Geophys. Res.,* **95,** 13 927–13 935.

Hansen, J., G. Russell, D. Rind, P. Stone, A. Lacis, S. Lebedeff, R. Ruedy, and L. Travis, 1983: Efficient three-dimensional global models for climate studies: Models I and II. *Mon. Wea. Rev.,* **111,** 609–662.

——, M. Sato, A. Lacis, R. Ruedy, I. Tegen, and E. Matthews, 1998: Climate forcings in the industrial era. *Proc. Nat. Acad. Sci. USA,* **95,** 12 753–12 758.

Haywood, J., and O. Boucher, 2000: Estimates of the direct and indirect radiative forcing due to tropospheric aerosols: A review. *Rev. Geophys.,* **38,** 513–543.

Lacis, A. A., and M. Mishchenko, 1995: Climate forcing, climate sensitivity, and climate response: A radiative modeling perspective on atmospheric aerosols. Environmental Science Research Rep. ES 17. *Aerosol Forcing of Climate,* R. Charlson and J. Heintzenberg, Eds., John Wiley and Sons, 11–42.

Liao, H., and J. Seinfeld, 1998: Radiative forcing by mineral dust aerosols: Sensitivity to key variables. *J. Geophys. Res.,* **103,** 31 637–31 645.

Liou, K.-N., 1986: Influence of cirrus clouds on weather and climate processes: A global perspective. *Mon. Wea. Rev.,* **114,** 1167–1199.

McClatchey, R. A., R. W. Fenn, J. Selby, and J. Garing, 1972: Optical properties of the atmosphere. Air Force Cambridge Res. Lab. Tech. Rep. AFCRL-72-0497, Bedford, MA, 113 pp.

Miller, R., and I. Tegen, 1998: Climate response to soil dust aerosols. *J. Climate,* **11,** 3247–3267.

Mishchenko, M. I., A. A. Lacis, B. E. Carlson, and L. D. Travis, 1995: Nonsphericity of dust-like tropospheric aerosols: Implications for aerosol remote sensing and climate modeling. *Geophys. Res. Lett.,* **22,** 1077–1080.

O'Brien, D., L. Rikus, A. Dilley, and M. Edwards, 1997: Spectral analysis of infrared heating in clouds computed with two-stream radiation codes. *J. Quant. Spectrosc. Radiat. Transfer,* **57,** 725–737.

Pierluissi, J., and G.-S. Peng, 1985: New molecular transmission band models for LOWTRAN. *Opt. Eng.,* **24,** 541–547.

Quijano, A., I. Sokolik, and O. Toon, 2000: Radiative heating rates and direct radiative forcing by mineral dust in cloudy atmospheric conditions. *J. Geophys. Res.,* **105,** 12 207–12 219.

Ricchiazzi, P., S. Yang, C. Gautier, and D. Sowle, 1998: SBDART: A research and teaching software tool for plane-parallel radiative transfer in the Earth's atmosphere. *Bull. Amer. Meteor. Soc.,* **79,** 2101–2114.

Ritter, B., and J.-F. Geleyn, 1992: A comprehensive radiation scheme for numerical weather prediction models with potential applications in climate simulations. *Mon. Wea. Rev.,* **120,** 303–325.

Schulz, M., Y. Balkanski, W. Guelle, and F. Dulac, 1998: Role of aerosol size distribution and source location in a three-dimensional simulation of a Saharan dust episode tested against sat-

ellite-derived optical thickness. *J. Geophys. Res.,* **103,** 10 579–10 592.

Sokolik, I., and G. Golitsyn, 1993: Investigation of optical and radiative properties of atmospheric dust aerosols. *Atmos. Environ.,* **27,** 2509–2517.

——, and O. Toon, 1999: Incorporation of mineralogical composition into models of the radiative properties of mineral aerosol from UV to IR wavelengths. *J. Geophys. Res.,* **104,** 9423–9444.

——, ——, and R. Bergstrom, 1998: Modeling the radiative characteristics of airborne mineral aerosols at infrared wavelengths. *J. Geophys. Res.,* **103,** 8813–8826.

Stamnes, K., S.-C. Tsay, W. Wiscombe, and K. Jayaweera, 1988: Numerically stable algorithm for discrete-ordinate-method radiative transfer in multiple scattering and emitting layered media. *Appl. Opt.,* **27,** 2502–2509.

Takara, E., and R. Ellingson, 2000: Broken cloud field longwave-scattering effects. *J. Atmos. Sci.,* **57,** 1298–1310.

Tegen, I., and A. Lacis, 1996: Modeling of particle size distribution and its influence on the radiative properties of mineral dust aerosol. *J. Geophys. Res.,* **101,** 19 237–19 244.

——, ——, and I. Fung, 1996: The influence on climate forcing of mineral aerosols from disturbed soils. *Nature,* **380,** 419–422.

Toon, O., C. Mckay, T. Ackerman, and K. Santhanam, 1989: Rapid calculation of radiative heating rates and photodissociation rates in inhomogeneous multiple scattering atmospheres. *J. Geophys. Res.,* **94,** 16 287–16 301.

Volz, F., 1973: Infrared optical constants of ammonium sulfate, Sahara dust, volcanic pumice, and flyash. *Appl. Opt.,* **12,** 564–568.

Wiscombe, W., 1980: Improved Mie scattering algorithms. *Appl. Opt.,* **19,** 1505–1509.